Optimizing final product properties and Ziegler-Natta catalyst performance with and without hydrogen in propylene polymerization by kinetic modeling

Gh. H. Varshouee[1], A. Heydarinasab[1*] A. Vaziri[1], B. Roozbahani[2]

[1] *Department of Chemical Engineering, Tehran Science and Research Branch, Islamic Azad University, Tehran, Iran*

[2] *Department of Chemical and Biomolecular Engineering, Research Associates of Rice University, USA*

Kinetics of propylene polymerization with its unique complexity has the key role on final product properties, but is heavily influenced by the hydrogen amount. Hydrogen, as chain-transfer agent, gives rise to a reduction of the average molecular weight of the polymer and directly affects the final product properties; and on the other hand, based on some theories up to a certain amount causes an increase followed by a decrease in the number of active sites. Therefore, this dual hydrogen behavior must be optimized. To date, no adequate kinetic model has been developed to predict and optimize this behavior and to simultaneously calculate the vital indices of final product properties such as melt flow index, number/weight average molecular weight, and polydispersity index. In addition to determining of the indices, by using the model some vital kinetic parameters such as activation energy, initial rate of reaction and deactivation constant can be easily calculated. The proposed model in this study was coded in MATLAB/SIMULINK software by using the polymer moment balance approach having in mind the dormant site theory as the most credible theory at the moment. The model was validated by comparison with lab experimental data and an agreement within the acceptable range of error was shown. Finally, the optimum reaction temperature and the optimum hydrogen amount according to the used catalyst were obtained as 70°C and 18 mg hydrogen in this study.

Keywords: Mathematical modeling, Propylene polymerization, Kinetic study, Hydrogen response, Population balance, Dormant site theory.

INTRODUCTION

Production of polypropylene (PP) is a multi-billion business, yielding more than 60 million metric tons of the polymer. Between 2005 and 2010, the average annual growth rate of polypropylene production has been about 6.5%/yr. Global polypropylene production capacity is expected to grow by 4.2%/yr from 2010 onwards [1]. With a view to the different applications of the polymer, different molecular weight distributions and final product properties are required; consequently, accurate control of the polymerization process is essential for adjusting appropriate final product properties. Hydrogen, as chain transfer agent, is one of the most important affecting factors on the reaction kinetics and final product properties. Up to now, despite of disputing on the role of hydrogen upon the polymerization, there is no validated mathematical model able to predict the kinetics and the end product simultaneously.

To date, most articles published in the field of polypropylene polymerization modeling have been concerned with heat and mass transfer inside the slurry polymer particles [2-4], or based on the mechanism of reaction and how multigrain particle grow according to [5-7]. Other studies have only concentrated on loop reactors [8,9] and fluidized-bed reactors (FBRs) [10,11], namely bulk and gas phase polymerization that are not applicable to a slurry reactor. As regards rate profiles of propylene polymerization, the first article on liquid phase (i.e. bulk polymerization, no slurry) was published by Samson *et al.* [12] and a number of other authors investigated the hydrogen effect on the kinetics [13-15].

Al-haj *et al*. [15] have observed a hydrogen effect on the profile of the polymerization curve of propylene polymerization in a liquid pool. Their research work was based on experimental results and did not provide a mathematical model. In relation to investigating hydrogen effect during propylene polymerization, many experimental studies have been carried out, but the results of these studies have been ambiguous and even contradictory. This means that the introduction of hydrogen gas during propylene homo-polymerization with Ziegler-Natta catalysts affects the polymerization rate, which can decrease, increase, or remain unaffected (Albizzati *et al.*) [16].

Guastalla & Gianinni, [17] showed that the initial rate of propylene polymerization reaches

---

asymptotically about 2.5 times the activity without hydrogen as hydrogen partial pressure is increased, whereas the deactivation rate decreases. Spitz *et al*. [18] found that low hydrogen concentrations in the reactor cause an enhancement of the rate profile; higher hydrogen levels lowered activity and increased deactivation. Rishina *et al*. [19] showed that there is a similar activation effect of hydrogen and found that the effect is reversible. Many researchers reported a similar hydrogen activation effect for different catalyst types and polymerization media [11,19-23]. Contrary to these findings, Soga & Siona [24] found that for $TiCl_4/MgCl_3/Al(C_2H_5)_3$/ethyl benzoate, the propylene polymerization rate decreases with increasing hydrogen partial pressure. According to the authors this is due to the slow addition of the monomer to the catalyst-hydrogen bond formed in the step of chain transfer to hydrogen. Similarly, Kahnnan *et al*. [25] made the conclusion that using a prepolymerized $TiCl_3/Et_2AlCl$ catalyst system, hydrogen not only has no effect on the polymerization rate for low hydrogen concentrations but the rate of polymerization decreases at a high hydrogen concentration; because adsorbed hydrogen lowers the effective monomer concentration near the catalytically active sites. Van Putten [10] pointed out that when hydrogen mole fraction exceeds the value of 0.011, gas-phase propylene polymerization rate starts to decrease. However, when hydrogen concentration is between 0 and 0.011?, a considerable increase in the polymerization rate is observed. According to the author, the decrease in the polymerization rate is due to the slow addition of the monomer to the catalyst-hydrogen bond formed in the step of chain transfer to hydrogen. The author further modeled the polymerization rate and the quasi-single site termination probability as a function of hydrogen-to-propylene molar ratio based on the dormant site theory [15]. Nevertheless, up to now, disputing continues. Luo *et al*. (2013) have modeled loop propylene polymerization reactors in bulk media [26]. The model focused on commercial reactor variables without paying attention to kinetics and final product properties. Next year, another paper has been published on modeling multi-scale PP properties, but in an FBR reactor [27]. In 2016, Seong *el al*. simulated liquid polypropylene polymerization reactors based on Spheripol technology [28]. Although they have paid attention to some final product properties such as average molecular weight and polydispersity, it was not suitable for kinetic study and predicting final product properties.

By means of profile polymerization rate operating conditions, the constancy of the reactor system and quality control of final product can be investigated and indicated, in particular, while hydrogen exists in the reactor system. Given that the effect of hydrogen on the reactor is still vague, a validated model of profile polymerization rate that could correctly predict the system is inevitable. Despite the importance of the matter, a few investigations have been devoted to this subject and no validated model was presented.

The aim of this work is to present a validated model for predicting profile polymerization rate, the effect of hydrogen concentration on profile rate, calculating the model of fraction activated sites catalyst *via* hydrogen concentration and determining important kinetic parameters such as (Ea, Ep, Rp0, Kd). In addition, the model is capable of calculating the most important final product indices, such as melt flow index (MFI), number average molecular weight (Mn), weight average molecular weight (Mw) and polydispersity index (PDI). In addition, the other purpose of this paper is to reveal the effect of hydrogen content on the fraction of activated catalyst sites during polymerization. The model was implemented in a MATLAB/SIMULINK environment and was validated with experimental data in slurry polymerization and the hydrogen response on the kinetic reaction was investigated. The global errors between the model outputs and experimental data are in an acceptable range.

EXPERIMENTAL

Materials

The 4th generation of spherical $MgCl_2$ supported Ziegler-Natta catalyst containing 3.6 wt% of Ti and diisobutyl phthalate (DIBP) as internal donor was supplied by Südchemie, Germany. Triethylaluminium (TEA of 98% purity) from Merck, Germany, diluted in n-heptane, used as co-catalyst and the so-called external donor (cyclohexyl methyl dimethoxy silane) were purchased from Merck and were used without further purification. Polymer grade propylene was provided by Shazand Petrochemical, Iran and was used as received. Hydrogen and nitrogen used were of >99.999% purity. Nitrogen was further purified by passing over beds of absorbents.

Polymer synthesis

In this study, slurry homopolymerization was carried out in heptane medium. Polymerization reactor was a 1L stainless steel vessel manufactured by Büchi Co.; polymerization set-up was designed

in order to conduct slurry polymerization in one vessel. A schematic diagram of the polymerization set-up is shown in Fig 1. A high pressure N_2 line was used to transfer liquid monomer and catalytic system into the reactor.

Catalyst system was injected to the reactor through a stainless steel cylinder in N_2 atmosphere. All gases were online purified by passing through three purification trains (containing molecular sieves) in a series. The individual gases were then filtered and the flow of each reactant was measured and controlled with a mass flow controller manufactured by Brooks.

Experimental R_p-t curves were recorded, the molecular weights of products were measured by gel permeation chromatography (GPC), employing an Agilent PL-220 model with TSK columns at 155°C using 1,2,4-trichlorobenzene as a solvent. The GPC was calibrated with narrow molecular weight distribution polystyrene standard as a reference. MFI of samples were evaluated according to ASTM 1238 at a temperature of 230ºC and load of 2.16 kg.
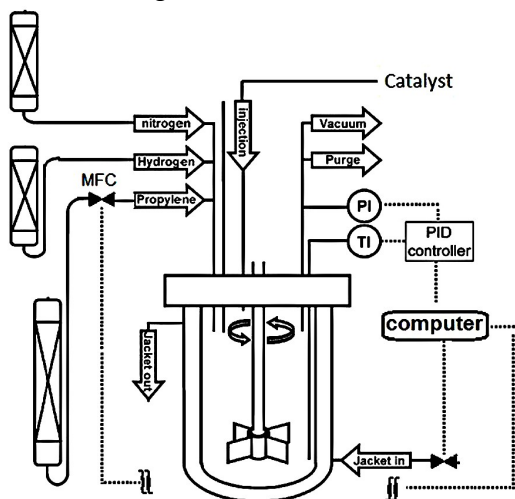

Figure 1. Simplified scheme of the reactor system.

Polymerization procedure

A typical polymerization procedure consisted of reactor preparation, polymerization and discharge. Details are as follows:

Firstly, the reactor was flushed with nitrogen gas at 90°C for 1 h and the reactor temperature was reduced to 20°C, then purged with propylene gas for 15 min. Afterwards, 500 ml of heptane as a solvent was introduced to the reactor; all inputs and outputs of the reactor were closed and stirring at 200 rpm for 5 min was performed for solvent degassing using a vacuum pump. Subsequently, hydrogen was entered to the reactor (based on recipe conditions), then propylene was introduced to the reactor according to controller program, then

the reactor was heated up to equilibrium thermodynamic conditions (T=70°C, Pr = 7.5 bar), finally the reactor was ready for catalyst injection to start polymerization. Injecting catalyst to the reactor was carried out under pressure *via* an injection system during polymerization time (two hours) at constant temperature and pressure, that is to say, the reaction was executed under isothermal and isobaric reactor conditions. Data were collected every five seconds.

It is worth mentioning that catalyst preparation should be done according to recipe in a glove box in a nitrogen atmosphere 20 min before injection to the reactor. After each experiment, the resulting polymer was dried under ambient conditions in a laboratory hood for 24 h.

Modeling description

Assumptions: The following modeling assumptions were considered:

1. It was supposed that propylene polymerization was carried out in an amorphous phase and amorphous phase concentrations during polypropylene polymerization were at the thermodynamic equilibrium conditions obeying Sanchez and Lacombe Equation (SLE) [29] for calculating the amount of X, the hydrogen molar ratio Eq (52).

2. It was assumed that $\gamma_1= \gamma_2=\cdots= \gamma_{NC,}$ where γ is equilibrium constant and NC is number of solvent in slurry phase components.

3. The reaction temperature, pressure and monomer concentration were kept constant during the polymerization process.

4. The resistances of both mass and heat transfer and the diffusion effect of the reactants were ignored.

5. It was assumed that the propagation constant is independent of the length of the growing polymer chain.

6. "Dormant sites theory" for activating catalyst by hydrogen concentration was used [15].

Formulation

As olefin polymerization kinetics with Ziegler-Natta catalysts might be fairly complicated, to date, several reaction steps have been proposed in the literature [9,10,12,18]. However, the most comprehensive steps were proposed by Zacca [9]. The ODE mass balance equations used in the model are (1)-(4). Since the model is a semi-batch process and constant monomer concentration during the polymerization is assumed, the input and output terms (Q_f and Q_0) are eliminated, then the terms of η and ζ are meaningless for our study.

The concentration variations with time used in he modeling are as follows:

$$C_j = C_H, C_A, C_E, C_{Mi}, C_B, C_S, C_T, C_{cat}, P_0^k, \mu_0^k, \mu_1^k, \lambda_0^k, \lambda_1^k, \lambda_2^k$$

The basic kinetic model used in this work is a simplified kinetic mechanism based on Zacca proposal [9] for semi-batch polymerization.

Therefore, in this work, our model is based on twelve of the most important reactions R5-16 and according to the dormant sites theory [15] the reactions R17-20 for hydrogen response model, as shown below:

$$\frac{dC_{j,R}}{dt} = [\frac{Q_f C_{j,f}}{V_R}]_{feed(input)} - [\frac{(\eta/\zeta)Q_0 C_{j,R}}{V_R}]_{output} + R_j \tag{1}$$
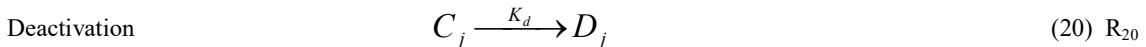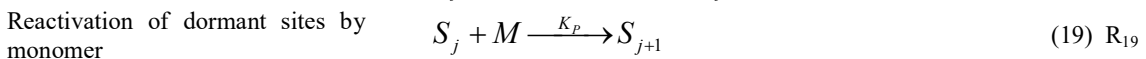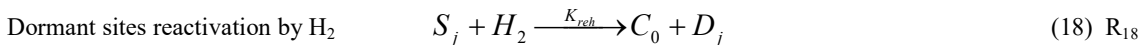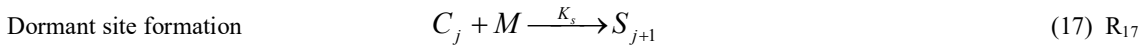
$$C_{j,R} = \frac{Mole \ \ of \ j}{Total \ \ Volume} \qquad\qquad for \ j = 1,2,....,NC \tag{2}$$

$$\eta_j = \frac{C_{j,a}}{C_{j,l}} \qquad\qquad for \ j = 1,2,....,NC \tag{3}$$

$$\zeta_j = \frac{C_{j,o}}{C_{j,R}} = \frac{\rho_0}{\rho_R} \cdot D_f \qquad where: \qquad (\eta/\zeta) = \begin{cases} \eta \ \ for \ \ liquid \ \ phase \ \ components \\ \\ \zeta \ \ for \ \ solid \ \ phase \ \ components \end{cases} \tag{4}$$

Reaction Step	Component	Reaction	Rate Equation	Reaction No
Site activation	Hydrogen	$C_p + H_2 \rightarrow P_0^K$	$R_{aH}^K = k_{aH}^k C_p C_{H,a}^{O_{aH}^K}$	(5) R₁
	Al-alkyl	$C_p + A \rightarrow P_0^K + B$	$R_{aA}^K = k_{aA}^k C_p C_{A,a}^{O_{aA}^K}$	(6) R₂
	Monomer i	$C_p + M_i \rightarrow P_0^K + M_i$	$R_{aMi}^K = k_{aMi}^k C_p C_{Mi}^{O_{aMi}^K}$	(7) R₃
Chain initiation	Monomer i	$P_0^k + M_i \rightarrow P_{\delta_i,i}^K$	$R_{P0i}^K = k_{P0i}^k P_0^K C_{M_i,a}$	(8) R₄
Chain propagation	Monomer j	$P_{n,i}^K + M_j \xrightarrow{Kp} P_{n+\delta_j,j}^K$	$R_{Pji}^K = k_{Pji}^k P_{n,j}^K C_{M_j,a}$	(9) R₅
Chain transfer	Hydrogen	$P_{n,i}^K + H_2 \xrightarrow{Kh} P_0^K + D_n^k$	$R_{cHi}^{K,n} = k_{cHi}^k P_{n,i}^K C_{H,a}^{O_{cHi}^K}$	(10) R₆
	Monomer j	$P_{n,i}^K + M_j \xrightarrow{Km} P_{\delta_j,j}^K + D_{r_i}^j$	$R_{cMji}^{K,n} = k_{cMji}^k P_{n,i}^K C_{j,a}^{O_{cMj,i}^K}$	(11) R₇
Site deactivation	Hydrogen	$P_{n,i}^K + H_2 \rightarrow C_d + D_n^k$	$R_{aHi}^{K,n} = k_{dH}^k P_{n,i}^K C_{H,a}^{O_{dH}^K}$	(12) R₈
		$P_0^K + H_2 \rightarrow C_d$	$R_{dH0}^K = k_{dH}^k P_0^K C_{H,a}^{O_{dH}^K}$	(13) R₉
	Al-alkyl	$P_{n,i}^K + A \rightarrow C_d + D_n^k$	$R_{dAi}^{K,n} = k_{dA}^k P_{n,i}^K C_{A,a}^{O_{dA}^K}$	(14) R₁₀
	Spontaneous	$P_{n,i}^K \rightarrow C_d + D_n^k$	$R_{dSpi}^{K,n} = k_{dSp}^k P_{n,i}^K$	(15) R₁₁
		$P_0^K \rightarrow C_d$	$R_{dSp0}^K = k_{dSp}^k P_0^K$	(16) R₁₂

Using dormant sites theory [15]:

Dormant site formation	$C_j + M \xrightarrow{K_s} S_{j+1}$		(17) R₁₇
Dormant sites reactivation by H₂	$S_j + H_2 \xrightarrow{K_{reh}} C_0 + D_j$		(18) R₁₈
Reactivation of dormant sites by monomer	$S_j + M \xrightarrow{K_P} S_{j+1}$		(19) R₁₉
Deactivation	$C_j \xrightarrow{K_d} D_j$		(20) R₂₀

The component rate equation [9] used in the model is as follows:

Hydrogen
$$R_H = -\sum_{K=1}^{Ns}[R_{aH}^k + R_{rH}^k + R_{dH0}^k + \sum_{i=1}^{Nm}\sum_{n=\delta_i}^{\infty}(R_{cHi}^{k,n} + R_{dHi}^{k,n})] \tag{21}$$

Co-catalyst
$$R_A = -\sum_{K=1}^{Ns}[R_{aA}^k + R_{dA0}^k + \sum_{i=1}^{Nm}\sum_{n=\delta_i}^{\infty}R_{dAi}^{k,n}] - R_{eA} \tag{22}$$

Electron donor
$$R_E = -\sum_{K=1}^{Ns}[R_{dE0}^k + \sum_{\substack{l=1\\l\neq K}}^{Ns}R_{tE0}^{kl} + \sum_{i=1}^{Nm}\sum_{n=\delta i}^{\infty}(\sum_{\substack{l=1\\l\neq K}}^{Ns}(R_{tEi}^{lk,n} + R_{dEi}^{k,n})] - R_{eE} \tag{23}$$

Poison
$$R_X = -\sum_{K=1}^{Ns}[R_{dX0}^k + \sum_{i=1}^{Nm}\sum_{n=\delta_i}^{\infty}R_{dXi}^{k,n}] - R_{eE} - R_{eA} \tag{24}$$

Potential sites
$$R_{Cp} = -\sum_{K=1}^{Ns}(R_{aH}^k + R_{aA}^k + R_{aSp}^k + \sum_{i=1}^{Nm}R_{aM_i}^k) \tag{25}$$

Vacant sites
$$R_{P_0^k} = R_{aH}^k + R_{aA}^k + R_{aSp}^k + \sum_{i=1}^{Nm}R_{aMi}^k + R_{rH}^k - R_{dH0}^k - R_{dE0}^k - R_{aA0}^k - R_{dSp0}^k - R_{dX0}^k - \sum_{j=1}^{Nm}R_{p0j}^k + \sum_{i=1}^{Nm}\sum_{n=\delta i}^{\infty}(R_{cHi}^{k,n} \cdot$$
$$+ \sum_{i=1}^{Nm}\sum_{\substack{l=1\\l\neq K}}^{Ns}\sum_{n=\delta i}^{\infty}(R_{tEi}^{lk,n} + R_{tSpi}^{lk,n})] + \sum_{\substack{l=1\\l\neq K}}^{NS}(R_{tE0}^{lk} + R_{tSp0}^{lk} - R_{tE0}^{kl} - R_{tSp0}^{kl}) \tag{26}$$

Dead sites
$$R_{Cd} = \sum_{K=1}^{Ns}[(R_{dH0}^k + R_{dE0}^k + R_{aA0}^k + R_{dX0}^k + R_{aSp0}^k - R_{rH}^k) + \sum_{i=1}^{Nm}\sum_{n=\delta i}^{\infty}(R_{dHi}^{k,n} + R_{dEi}^{k,n} + R_{dAi}^{k,n} + R_{dXi}^{k,n} + R_{dSpi}^{k,n})] \tag{27}$$

Monomer
$$R_{Mi} = -\sum_{K=1}^{Ns}[R_{P0i}^k + \sum_{j=1}^{Nm}\sum_{n=\delta i}^{\infty}(R_{Pij}^{k,n} + R_{cMi,j}^{k,n})] \tag{28}$$

Moments equations:

The moments equations for slurry polymerization of PP are presented:

Live polymer
$$R_{P_{n,i}^k} = \delta(n-\delta_i)[R_{P0i}^k + \sum_{j=1}^{Nm}\sum_{m=\delta i}^{\infty}R_{cMi,j}^{k,m}] + \sum_{j=1}^{Nm}k_{pij}^k C_{Mi,a}P_{n-\delta_i,j}^k - \sum_{j=1}^{Nm}k_{pij}^k C_{Mj,a}P_{n,i}^k - \alpha_i^k \tag{29}$$

Dead polymer
$$R_{D_{n,}^k} = \sum_{i=1}^{Nm}\alpha_i^k P_{n,i}^i \quad \text{where}$$
$$\alpha_i^k = k_{cHi}^k C_{H,a}^{O_{cHi}^k} + k_{cSpi}^k + \sum_{j=1}^{Nm}k_{cMj,i}^k C_{Mj,a} + \sum_{\substack{l=1\\l\neq K}}^{Ns}(k_{tEi}^{kl} C_{E,a}^{O_{tE}^{kl}} + k_{tSpi}^{kl}) + k_{dHi}^k C_{H,a}^{O_{dH}^k} + k_{dAi}^k C_{A,a}^{O_{dA}^k} + k_{dEi}^k C \tag{30}$$

Live moment
$$\mu_{\delta_i,i}^k = \sum_{n=1}^{\infty}n^{\delta_i}P_{n,i}^k \tag{31}$$

Bulk moment
$$\lambda_{\delta_i}^k = \sum_{n=\delta_i}^{\infty}(\sum_{i=1}^{Nm}P_{n,i}^k + D_n^k) \tag{32}$$

Zero-order live polymer moments
$$R_{\mu_{0,i}^K} = R_{P0i}^k + \sum_{j=1}^{Nm}k_{cM_i,j}^k C_{Mi,a}\mu_{0,J}^k - \alpha_i^k\mu_{0,J}^k + \sum_{j=1}^{Nm}[k_{pij}^k C_{Mi,a}\mu_{0,J}^k - k_{pji}^k C_{Mj,a}\mu_{0,i}^k] \tag{33}$$

First-order live polymer moments
$$R_{\mu_{\delta l}^K} = \sum_{i=1}^{Nm}\delta(i-l)[R_{P0i}^k + \sum_{j=1}^{Nm}k_{cM_i,j}^k C_{Mi,a}\mu_{0,J}^k] - \sum_{i=1}^{Nm}\alpha_i^k\mu_{\delta_i,i}^k + \sum_{i=1}^{Nm}\sum_{j=1}^{Nm}k_{pij}^k C_{Mi,a}\delta(i- \tag{34}$$

Zero-order bulk polymer moments
$$R_{\lambda_0^K} = \sum_{i=1}^{Nm}[R_{P0i}^k + \sum_{j=1}^{Nm}k_{cM_i,j}^k C_{Mi,a}\mu_{0,J}^k] \tag{35}$$

First-order bulk polymer moments
$$R_{\lambda_{\delta l}^K} = \sum_{i=1}^{Nm}\delta(i-l)[R_{P0i}^k + \sum_{j=1}^{Nm}k_{cM_i,j}^k C_{Mi,a}\mu_{0,J}^k] + \sum_{i=1}^{Nm}\sum_{j=1}^{Nm}\delta(i-1)k_{pij}^k C_{Mi,a}\mu_{0,J}^k \tag{36}$$

Second-order bulk polymer moments
$$R_{\lambda_2} = \sum_{K=1}^{Ns}\sum_{j=1}^{Nm}[R_{P0i}^k + \sum_{i=1}^{Nm}k_{cMj,i}^k C_{Mj,a}\mu_{0,i}^k] + \sum_{k=1}^{Ns}\sum_{i=1}^{Nm}\sum_{j=1}^{Nm}k_{pji}^k C_{Mj,a}(\mu_{0,i}^k + \tag{37}$$

The basic polymer properties, called end-use properties, are four items: number average molecular weight (Mn), weight average molecular weight (Mw), melt flow index (MFI) and polydispersity index (PDI).

The equations used in the model are as follows [9]:

$$\overline{M_n} = \sum_{K=1}^{Ns} \sum_{i=1}^{Nm} \frac{\lambda_{\delta_i}^k}{\lambda_0^k} \overline{M_i} \qquad (38)$$

$$\overline{M_w} = \lambda_2 \cdot \frac{\sum_{k=1}^{Ns} \lambda_0^k \overline{M_n}}{(\sum_{K=1}^{Ns} \sum_{i=1}^{Nm} \lambda_{\delta_i}^k)^2} \qquad (39)$$

Then: $DPI = \dfrac{\overline{M_w}}{\overline{M_n}}$ (40)

As the melt flow index is a function of molecular weight, the power-law-type equation below is suggested. Parameters a and b are calculated by fitting appropriate experimental data, it will be discussed later.

$$R_p = R_{p0} \bullet \exp(-k_d \circ t) \qquad (41)$$

Determination of the kinetic parameters

A typical polymerization rate profile (Figs. 6 and 7) is comprised of two areas; (I) initial polymerization start up zone, (II) quasi-steady-state zone [15].

Each zone has a significant meaning in kinetic analysis; detailed discussions of these issues have undergone a considerable debate and are not repeated here for the sake of brevity.

Pater *et al*. [13] and some other researchers [14, 15] have shown that the rate of polymerization at isothermal conditions can be described as a first-order process in monomer concentration and the deactivation of the catalyst as a first-order process in the number of active sites. The following equations are used:

$$R_p = K_p C_m C^* \qquad (42)$$

$$\frac{dC^*}{dt} = -K_d C^* \qquad (43)$$

Combination and integration for isothermal conditions leads then to the following expression that is often used in the literature to describe the time dependent rate of polymerization:

$$R_p = R_{p0} \bullet \exp(-k_d \circ t) \qquad (44)$$

So, for finding R_p at isothermal conditions, two parameters, namely R_{p0} and k_d should be obtained. R_{p0} and k_d are determined graphically by the profile of the polymerization rate curve, as shown in Fig. 2. These parameters depend on reaction temperature, hence according to Arrhenius equation, we have:

$$R_p = R_{p0} \bullet \exp(-\frac{E_a}{R.T}) \qquad (45)$$

$$k_d = k_{d0} \cdot \exp(\frac{-E_{a,d}}{RT}) \qquad (46)$$

Here, R_{p0} is the initial reaction rate, k_d the deactivation constant, $E_{a,d}$ the activation energy for the lumped deactivation reaction, t shows time, and T indicates the temperature. So it could be calculated from the profile of the rate curve of polymerization (t=0).

Since the rate of polymerization depends on temperature, having R_{p0} at different temperatures by using Arrhenius equation, the activation energy of any type of catalyst is easily predictable (as shown by the typical curve in Fig. 2).

Two very important issues should be considered about the activation energy of the Z-N catalyst: (1) it is independent of the hydrogen concentration [15] and (2) it is an intrinsic property of any catalyst and thus can be expected to differ from one type to another.

Yield of the polymerization can be calculated by integrating the rate.

$$Y_{calc} = \int_0^t R_P \cdot dt \qquad (47)$$

Amount of Y_{calc} is exactly equal to the area under the profile curve. If this value is multiplied by the weight of catalyst, the produced polymer will be obtained in each batch. Experimentally, the yield is measured by weighing the dry product of batch polymerization. But in fact, much more monomers (consumed monomer) are entered to the reactor, that a part of them are reacted and the other part have remained as unconverted monomer in liquid and gas phases. The model is capable of directly calculating yield and consumed monomer. By plotting the natural logarithm of the reaction rate *versus* polymerization time, a linear fit can be made where the slope of the fit line is k_d, and the intercept is R_{p0}. Fig. 2 illustrates the method.

Hydrogen effect and dormant sites theory to determine k_p

Propagation reaction is the most important reaction in polymerization. Accordingly, determining the value of constant (K_P) and activation energy (E_p) is inevitable for modeling. Before proceeding with discussions in this regard, it is necessary to understand dormant sites theory and the role of hydrogen in polymerization.
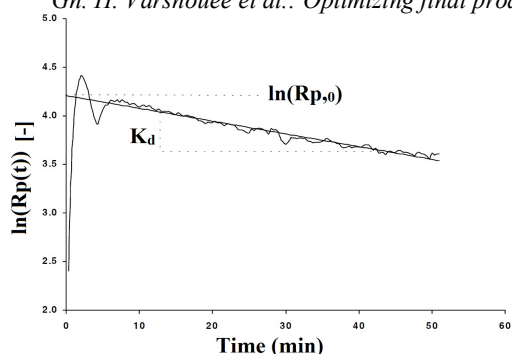
Figure 2. Determination of initial reaction rate R_{p0} and deactivation constant k_d.

Hydrogen always acts as a chain transfer agent during olefin polymerization; when the hydrogen concentration increases, the molecular weight of the polyolefin decreases. On the other hand, the effect of hydrogen on catalyst activity during olefin polymerization is less predictable and varies depending on the type of catalyst, monomer, and donor systems. For instance, hydrogen generally reduces the polymerization rate of ethylene and increases the polymerization rate of propylene when high-activity $TiCl_4/MgCl_2$ catalysts are used (Shaffer and Ray [4]). On the other hand, the effect of hydrogen on catalyst activity during olefin polymerization is less predictable and varies depending on the type of catalyst, monomer, and donor systems. For instance, hydrogen generally reduces the polymerization rate of ethylene and increases the polymerization rate of propylene when high-activity $TiCl_4/MgCl_2$ catalysts are used. So it is concluded that the hydrogen effect depends on two factors: (i) nature of catalyst system and (ii) monomer type. So far, three theories have been suggested to account for the increase in the value of the polymerization rate caused by hydrogen.

Theory 1: Increase in the number of active sites theory.

Theory 2: Change in oxidation states theory.

Theory 3: Dormant sites theory.

The former two theories have been discussed and rejected in the open literature [24,18] and are not repeated here for the sake of brevity.

According to the third, strongest theory so far, the hydrogen effect is illustrated in this statement. Since a propylene molecule is asymmetric with respect to the double bond, it has been suggested that monomers may insert at the catalyst site in four distinct arrangements (head to tail, tail to tail, tail to head and head to head).

Growing chains have two positions of dealing with other monomers (position 1-2 and position 2-1). If the growing chain reacts with position 2-1 of propylene, a "dormant site" will be created, as

shown in Fig. 4. Dormant sites are the drawback of propylene polymerization. Busico *et al.,* (1993) [30] have measured the distributions of end groups in polypropylene in the presence of hydrogen and have suggested that if the propylene molecule inserts in the 2-1 mode, the rate of propagation is reduced due to steric hindrance by the Ti atom. These results are supported by the end group analysis done by Chadwick *et al.* [31].

According to the dormant sites theory, increasing the hydrogen concentration decreases the concentration of dormant sites. The modeling of reaction kinetics and molecular weight is based on the dormant site mechanism (Weickert, 2002 [15]). A "quasi-single-site" model is applied to explain the average behavior of the active sites. In addition, it is assumed that all active sites have the same average rate constants. The chain transfer with co-catalysts is neglected and a quasi steady state is assumed for dormant sites.

This means that according to the dormant sites theory, the reactions R_{9-11} and R_{17-20} are the effective reactions on hydrogen response. Using the long chain hypothesis in addition to the assumptions mentioned earlier, the kinetics of Z-N catalysts can be described as a first-order function of both monomer concentration, C_m, and the concentration of active sites, C using a lumped propagation constant K_p.

$$R_p = K_p.C.C_m \tag{48}$$

In reality, the active sites are more or less covered by the polymer produced. The actual catalyst site concentration is between the maximum concentration of active sites C_{max}, and the concentration of dormant sites Cs:

$$C = C_{max} - C_S \tag{49}$$

The concentration of the dormant sites can be calculated assuming the quasi-steady-state:

$$R_S = 0 = K_s.C.C_m - K_{reh}.C_s.C_{H2} - K_{rem}.C_s.C_m \tag{50}$$

K_s, K_{reh} and K_{rem} are rate constants for dormant sites formation, dormant sites reactivation by hydrogen and monomer reactions respectively. So by rearranging these equations, it is concluded that:

$$C_s = \frac{K_s.C}{K_{reh}.X + K_{rem}} \tag{51}$$

where X is the hydrogen molar ratio defined as:

$$X = \frac{C_{H2}}{C_m} \tag{52}$$

Combining Equations (49) and (51) leads to:

$$C = \frac{C_{max}.(1+K_1.X)}{1+K_2+K_1 X} \qquad (53)$$

with

$$K_1 = \frac{K_{reh}}{K_{rem}} ; \quad K_2 = \frac{K_s}{K_{rem}} \qquad (54)$$

Based on this derivation, Equation (43) can be described as a function of three parameters, k_1, k_2 and k_p:

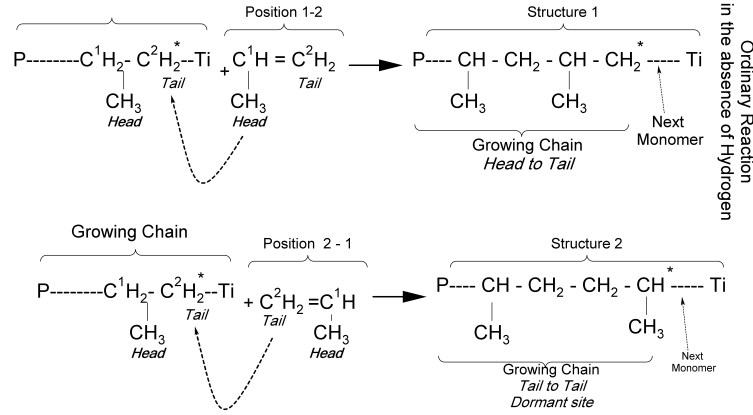$$R_p = \frac{K_p.C_m.C_{max}.(K_1.X+1)}{1+K_1.X+K_2} \qquad (55)$$

Figure 3. Dormant site generation

Equation (55) can be rewritten as:

$$R_p = K_p.C_{max}.C_m.f_{H_2} \qquad (56)$$

with the hydrogen-dependent function f_{H2} defined as:

$$f_{H_2} = \frac{1+K_1.X}{1+K_2+K_1.X} \qquad (57)$$

The parameter f_{H2} represents the fraction of active sites in system. In the absence of hydrogen X = 0, and f_{H2} has a minimum value. This means that the active sites of catalyst are at minimum level in the polymerization system. Consequently, if $f_{H2,max}$ = 1, 100 % of the catalyst sites are active in the reaction.

Equation (57) has three parameters to be determined, namely k_p, k_1, and k_2 The fit is done in two steps, in the first step the value of $(k_p/(1+k_2))$ is obtained, then the values of k_1 and k_2 are estimated. The first step: As the active sites of the catalyst are heterogeneous, the calculated k_P is an average value. This value is determined using the experiments without hydrogen, runs 1, 2 and 3. When no hydrogen is used in the experiments, Eq (55) can be rewritten as:

For X=0 (no hydrogen)

$$R'_{p_0} = \frac{K'_p}{1+K_2}.\rho_m \qquad (58)$$

where R'_{p_0} [mol/l sec] and R_{p_0} [kg/g$_{cat}$.h], and with rearrangement we have:

$$R_{p_0} = \frac{R'_{p_0}}{\rho_m} = \frac{K_p'}{1+K_2} \qquad (59)$$

Based on these results, the dependency of $(k_p/1+k_2)$ on reaction temperature has the following form:

$$K_p = K_{p_0}.(1+K_2).\exp(-\frac{E_p}{R.T}) \qquad (60)$$

Then we have:

$$Ln(\frac{R_{p_0}}{\rho_m}) = Ln(\frac{K_p}{1+K_2}) = Ln(K_{p_0}) - \frac{E_p}{R.T} \qquad (61)$$

Here ρ_m is the monomer density. The Arrhenius plot for $(k_p/l+k_2)$, Fig. 9, shows an excellent fit with linear correlation coefficient (R^2) of 0.9967.

MODELING ALGORITHM

Fig. 4 presents the algorithm of the model solution in a MATLAB/SIMULINK environment. It is composed of two parts; main-program (named "Runsim") and subroutine (function file).

In this study, as in the available literature [8,9], the initially guessed kinetic constants were applied to the model and afterward were adjusted and the exact values were determined for the polymerization according to the set-up (experimental data) by the iterative methodology, as shown in Fig. 5.

RESULTS AND DISCUSSION

Comparison of the model outputs and experimental results in different conditions is summarized in Table 1. The model was validated by experimental data (as shown in Fig. 6(a) in the absence of hydrogen at different temperatures and in Fig. 7 at a constant reactor temperature (70ºC) with different hydrogen concentrations). As it can be seen, the experimental results and model outputs were within an acceptable margin of errors. The margin of errors was determined by:

1. Global error that is the summation of truncation, method and round off error;
2. Personal and measurement equipment errors;
3. Selection of Equation of state.
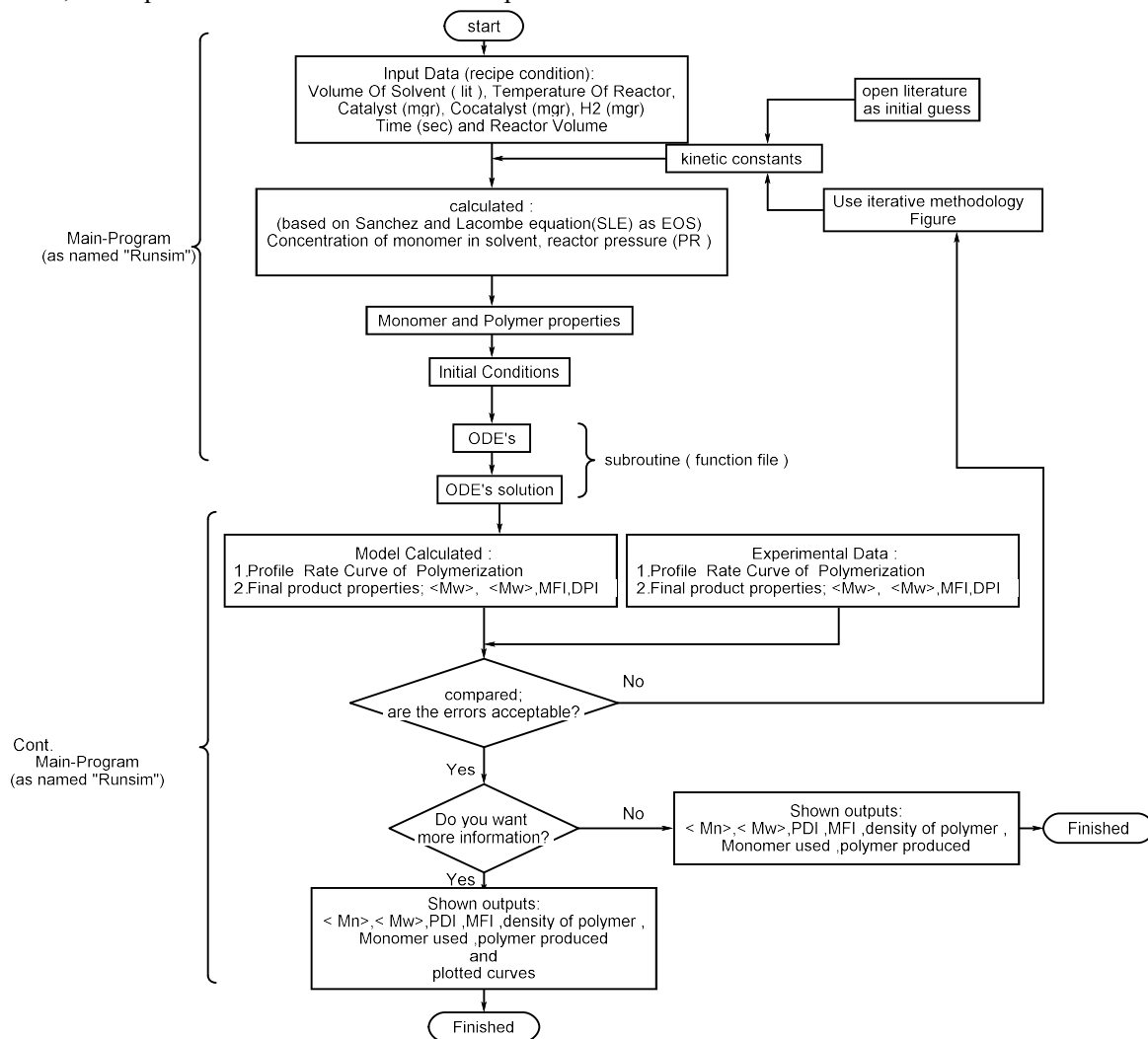4. Errors resulting from assumptions.

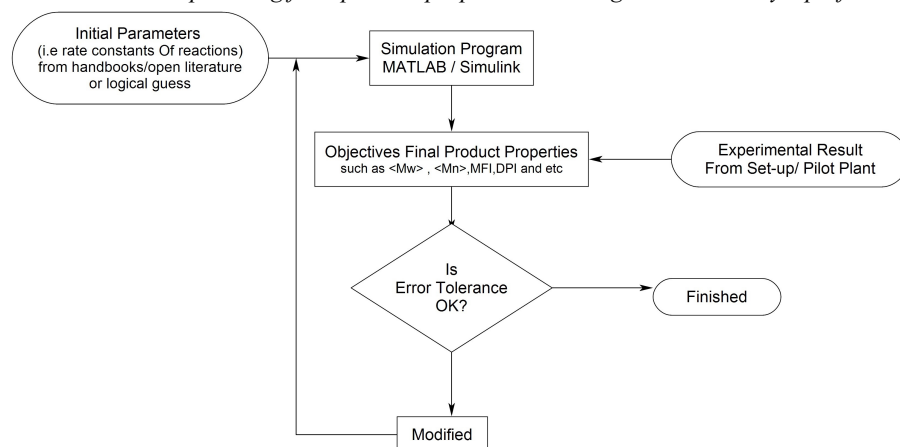**Figure 4.** The general algorithm modeling in this work

Figure 5. The iterative methodology used to adjust kinetic parameters (constants) in this work.

Table 1. Summarized polymerization recipe; Model and experimental output results

Recipe					Results (Experimental / Model)							
Run No.	T (°C)	H2 (mg)	Catalyst (mg)		Y (gram)	Rp0	Kd (1/hr)	<Mn>	<Mw>	PDI	MFI	ρ (Kg/m^3)
1	65	0	20	Exp. R[1]	63.29	5.01	1.42	210259	863057	4.1	0.75	
				Mod. R[2]	65.13	5.19	1.42	205570	834523	4.06	0.81	589.44
2	70	0	20	Exp. R	72.66	6.5	1.95	304642	1104374	3.63	0.42	
				Mod. R	76.4	7.46	1.98	323780	1214440	3.75	0.33	619.37
3	75	0	20	Exp. R	63.07	8.85	2.04	236154	1124367	4.76	0.4	
				Mod. R	67.25	8.92	2.13	270243	1178300	4.36	0.36	614.62
4	70	183	10	Exp. R	81.33	11.24	2.27	29962	144192	4.81	37	
				Mod. R	88.4	11.43	2.3	32812.7	148874	4.54	36.99562	637.11
5	70	274	10	Exp. R	74.61	11.02	2.05	24016	116939	4.87	62	
				Mod. R	76.81	11.2	2.35	24981.1	123303	4.94	61.98627	620.01
6[6]	70	2000[5]	10	Exp. R								
				Mod. R	64.92	9.34	2.81	9952.25	70163.4	7.06		
7[7]	70	2500[8]	10	Exp. R								
				Mod. R	61.26	8.74	2.97	8353.86	61651.5	7.38		

X: Hydrogen molar ratio calculated by Aspen Software polymer software based on SLE (SOE). [1] Experimental result, [2] Model result, [3] 18 mg H_2 is equivalent to 0.00466 molar ratio X, [4] 27 mg H_2 is equivalent to 0.00703 molar ratio X, [5] 2000 mg H_2 is equivalent to 0.0206 molar ratio X, [6] Mathematically calculated. But in fact, this product is off or wax grade, [7] 2500 mg H_2 is equivalent to 0.0243 molar ratio X, [8] Mathematically calculated. But in fact, this product is off or wax grade.

After validating the model, the data of runs 6 and 7 come from model for checking the performance of model and calculating some kinetic parameters such as K_1 for Eq (57) to modeling f_{H2}.

The results of the model are in line with what was expected.

The results of Table 1 demonstrated that in the absence of hydrogen, the polymerization rate increased up to 70°C and then decreased at 75°C.

This claim can be verified by investigating the yield of products because the polymerization rate has a direct impact on the yield. Meanwhile, increasing reaction temperature leads to increased deactivation constant (K_d) of the catalyst (Table 1). Accordingly, this event is an important constraint of the reaction. Deactivation of the used catalyst as a function of temperature can be interpreted by Fig. 6 (b) and (c). From Fig. 6 (b) it can be seen that the rate of polymerization at the highest temperature (75°C) sharply increases to the peak in the initial zone, then rapidly drops to point A (about half an hour after beginning the reaction). Hence forward the rate gradually decreases until one hour after starting polymerization and hereafter, it is in a steady condition. So it is concluded that, in the first half hour of the reaction, the catalyst loses most of its activities and after one hour, its activity is at the least possible. This event is not very favorable, and it is a drawback of the process conditions. The profile rate of polymerization at 70°C is the most favorable one, since firstly, it provides the highest yield, and secondly, the catalyst deactivation rate is more acceptable than the other. Therefore it is concluded that 70°C is the optimum reactor temperature. The decrease in polymer yield at the higher temperature is due to catalyst deactivation ether by overreduction of the catalyst sites or *via* an alkylation process with the Lewis base [12].

In order to investigate the effect of variable hydrogen concentration on the profile polymerization rate, Fig. 7 was plotted at the optimum reactor temperature (70°C). To verify the performance of the model, Fig. 7 compares the experiment with the model profile polymerization rate. It is seen that each of both profile rates in same conditions have a fairly good consistence with each other in an acceptable margin of error. The error margin of the final product properties such as Mw, DPI and MFI between model output results and experimental data is acceptable as well (*cf.* Table 1). Accordingly, it is concluded that the model is validated.

It is worth mentioning that according to Arrhenius equation, Ea is dependent on temperature and independent on hydrogen concentration [15]. Therefore, activation energy was calculated by Eq (45) and Fig. 8. It is notable that the activation energy obtained in this work is in line with the open literature data as shown in Table 2. From Fig. 9, the constants of equation (41) could be estimated for predicting MFI by average MW.

Since the most reactions in the polymerization belong to propagation reactions, as expected, the overall activation energy Ea should be very close to the propagation activation energy Ep. Therefore, with calculating and comparing Ep with Ea at least error, it could be a criterion of the accuracy and validity of the model.

Ep was calculated by means of dormant site generation theory using Eq (61) and plotting in Figure 8. The figure shows an excellent fit with linear correlation coefficient (R^2) of 0.9967. Then, from the slope of the line in Fig 10, Ep is obtained. It is interesting to note that comparing Ea and Ep , the difference is only 4% error (Table 3). This is another reason that the model was well enough validated. In addition, the dormant site generation theory is accurately justified by the profile curve rate of propylene polymerization.

In this respect, Al-haj *et al.* (2007), using experimentally method in liquid pool media, have calculated Ea and Ep with approximately 12.82% error (*cf.* table 2). Therefore, this error difference has a significant effect on the subsequent calculations such as R_{p0}, K_1 and K_2 (summarized in Table 3).

Using the dormant theory, equation (57) is obtained. On the other hand, K_1 and K_2 can be estimated using the output of the model and Fig. 8. The equation predicts the fraction of the catalyst active sites *via* hydrogen molar ratio (X). For instance, if there is no hydrogen in the polymerization system (X=0), only 10% of the potential of the catalyst is active, and about 90% of it is laid down and unused (Fig. 9 a). The impact of this issue on Y and R_{p0} is exactly clear and the model is able to predict that (*cf.* Fig. 6 b,c,d,e,f and table 1). Then, by slightly increasing hydrogen content such as X=0.00466, the fraction of activated sites of the catalyst rapidly increases (85.5%) (Figs. 7 and 11 a). But the increasing hydrogen content caused an increase in the deactivation constant K_d (Fig. 11 c). This is not desirable due to the quick deactivation of the catalyst. On the other hand, the increasing hydrogen content has an inverse effect on R_{p0} and Y, in other words, it may lead to changing final product properties and even producing off grade or wax product (Fig. 11 b and d).
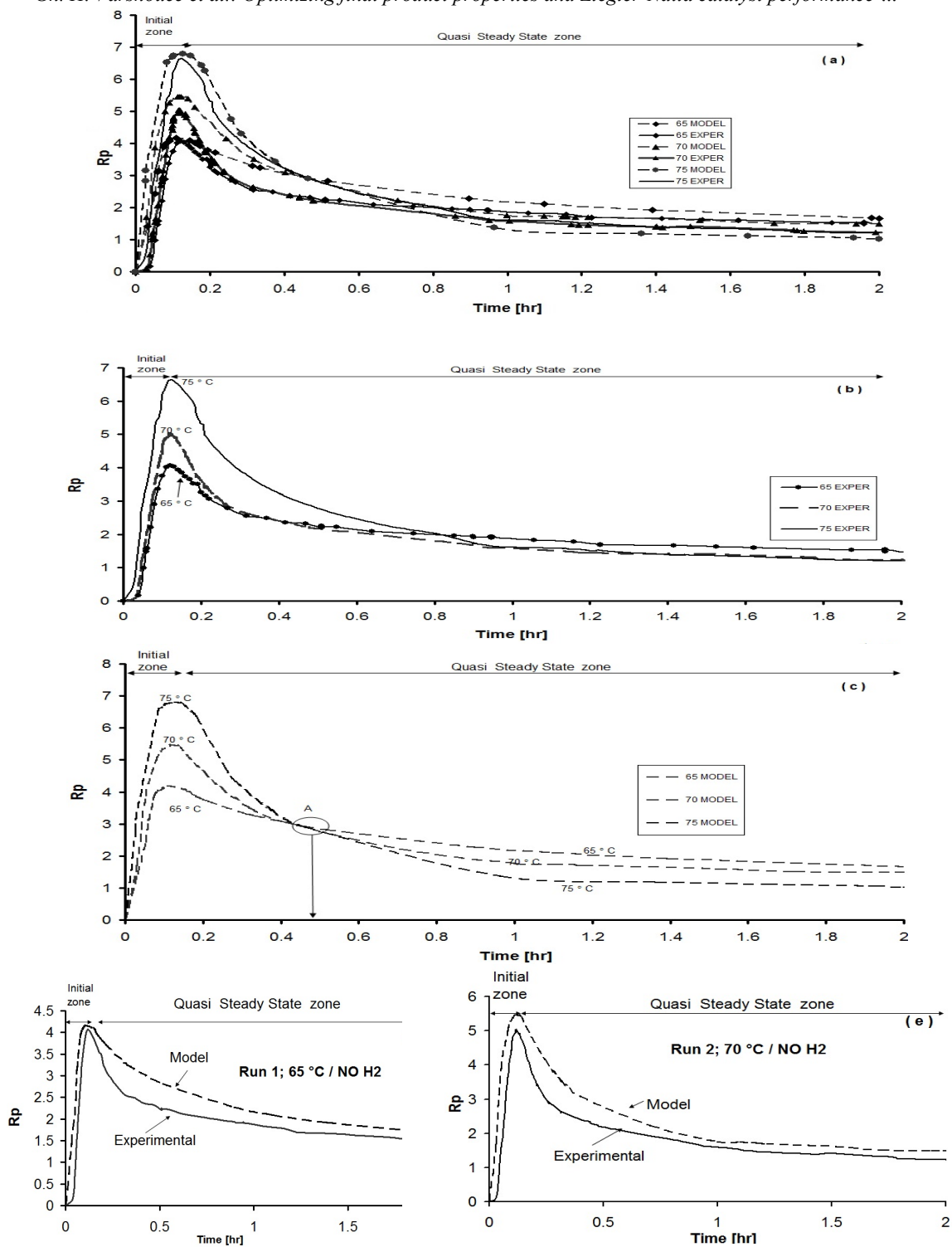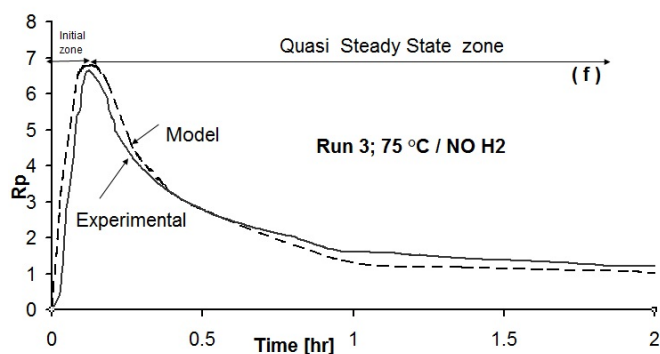
Figure 6. Comparison of experimental and model profile rate in the absence of hydrogen at different temperatures. (a) comparison of model and experimental altogether; (b) comparison of all experimental runs (1,2,3) altogether; (c) comparison of all model runs (1,2,3) altogether; (d) comparison of model and experimental run 1; (e) comparison of model and experimental run 2; (f) comparison of model and experimental run 3.
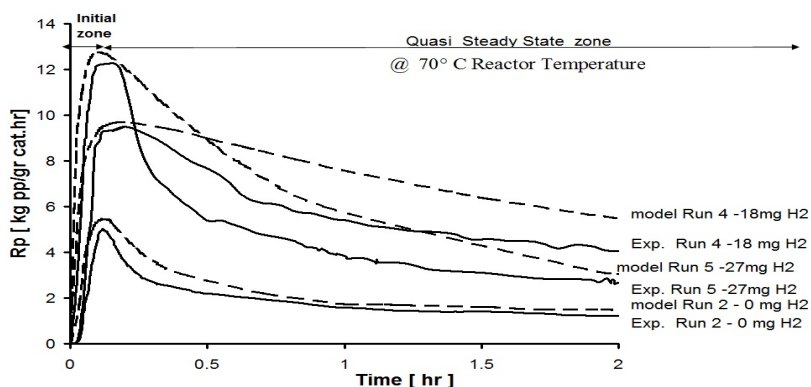

Figure 7. Comparison of experimental and model profile rate in the presence of different hydrogen concentrations at a constant temperature of 70°C.
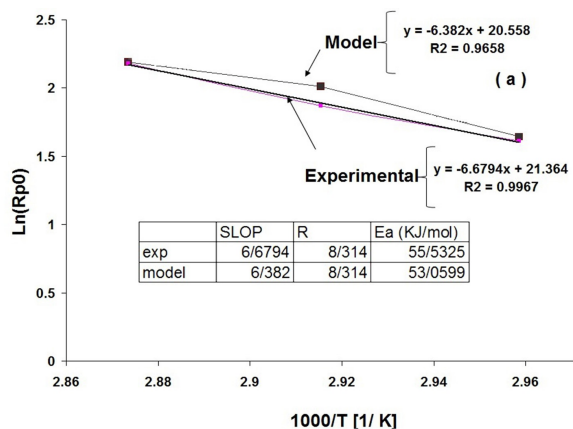

	SLOP	R	Ea (KJ/mol)
exp	6/6794	8/314	55/5325
model	6/382	8/314	53/0599

$y = -6.382x + 20.558$
$R2 = 0.9658$

$y = -6.6794x + 21.364$
$R2 = 0.9967$

$Log(MFI) = -2.3757 \, Log(MW) + 13.977$
$R^2 = 0.9998$
then, for this study

$MFI = a \cdot (\overline{M_w})^b$
$a = 9.4841 \times 10^{13}$
$b = -2.3747$

Eq (41)

Figure 8. Obtaining Ea by Arrhenius plot of the initial polymerization rates R_{p0} at different temperatures
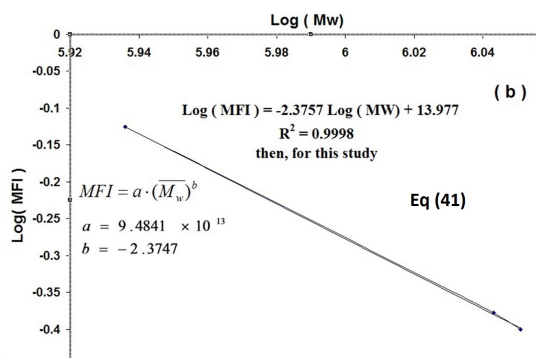
Figure 9. Obtaining constants of eq (42), relation of Mw with MFI

$$Ln\left(\frac{R'_{p0}}{\rho_p}\right) = -\frac{6.6894}{T} + 17.663$$
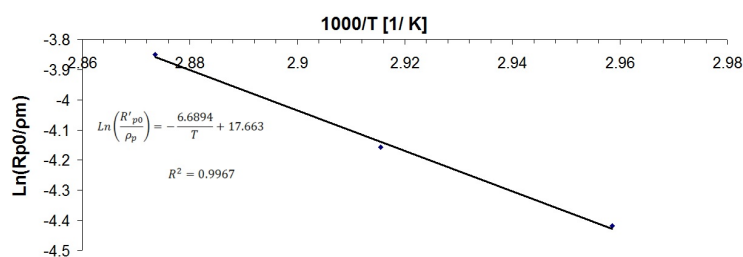
$$R^2 = 0.9967$$

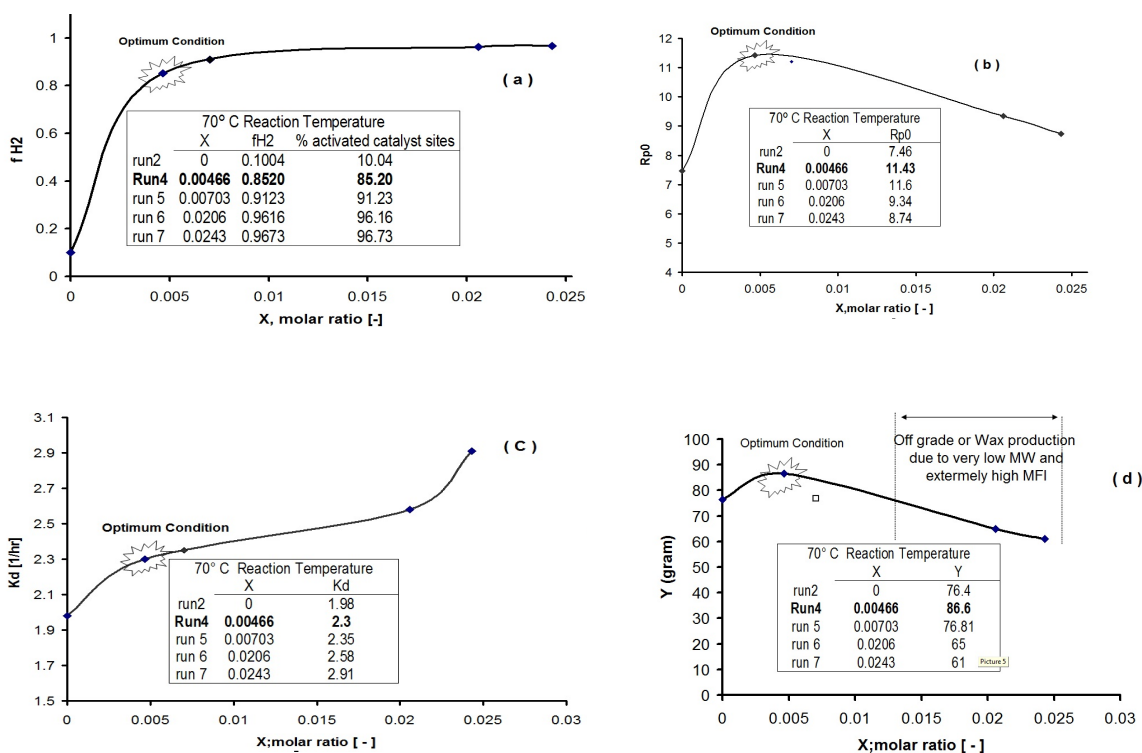**Figure 10.** Calculation of propagation constant by using Eq (61)

Figure 11. Effect of various hydrogen concentrations on the kinetic parameters: (a) f_{H2}; (b) R_{p0}; (C) K_d; (d) Yield

Table 2. Comparison of reported activation energies (Ea) in propylene polymerization systems.

Worker	Catalyst System	Phase	Ea, (KJ/mol)	Reference
Yuan *et. al.*	δ-TiCl$_3$. 1/3 AlCl$_3$ /DEAC	Slurry	53.9	32
Soares *et. al.*	TiCl$_3$/DEAC	Slurry	57.7	20
Al-haj *et al.*	MgCl$_2$/TiCl$_4$/phthalate/silane/TEA	Liq. pool	58.6	15
This work (ave)	MgCl$_2$/TiCl$_4$/phthalate/silane/TEA	Slurry	55.53	*This paper Exp.*
This work (ave)	MgCl$_2$/TiCl$_4$/phthalate/silane/TEA	Slurry	53.05	*This paper Model.*

CONCLUSION

In this paper, a validated mathematical model based on moment approach for an isothermal slurry polymerization of propylene with Ziegler-Natta catalysts is presented that is able to calculate the most important indices of end used product, such as melt flow index (MFI) , number average molecular weight (Mn), weight average molecular weight (Mw) and polydispersity index (PDI), and hydrogen response of the propylene polymerization system.

The model output was in good agreement with experimental results and revealed that there was an optimum temperature (70°C) and hydrogen concentration (18 mg) to achieve maximum amount of polymer yield. At the optimum temperature the PDI was at minimum, indicating optimum dispersity of the polymer chains. In absence of hydrogen, an increase in temperature led to reduction of molecular weight and enhancement of MFI. The activation energy did not depend on the presence or absence of hydrogen and hydrogen

concentration. The model could be able to predict deactivation constant of a unknown catalyst in the presence or absence of hydrogen in the polymerization system.

Table 3. Comparison of kinetic constants in this work with literature data.

	Condition	Overall Ea [kJ/mol]	Ep [kJ/mol]	Err. %	K_{p_0} $[m^3 / gr_{cat}.hr]$	$K_{2[-]}$
Al-haj *et al.* [15] Slurry-bulk	Liquid pool	58.6	67.22	12.82	6.41×10^8	8.02
	$K_1 = -32.2 \cdot T^2 + 2.26 \cdot T - 3.86 \times 10^6$					
	Catalyst system: MgCl$_2$/TiCl$_4$/phthalate/silane/TEA					
This work	Slurry in heptane	53.0599	55.61	4.5	4.69×10^6	8.97
	$K_1 = -1.529 \cdot T^2 + 555.24 \cdot T - 4.226 \times 10^6$					
	Catalyst system: MgCl$_2$/TiCl$_4$/phthalate/silane/TEA					

Notation:

C total active site concentration, kgmol/m^3
C_d dead-site concentration, kgmol/m^3
C_j component *j* bulk concentration, kgmol/m^3
    component *j* concentration at amorphous polymer phase
$C_{j, a}$ (effective concentration), kgmol/m^3
$C_{j,f}$ component *j* concentration at feed stream, kgmol/ m^3
$C_{j,l}$ liquid-phase concentration of component *j*, kgmol/ m^3
$C_{j,R}$ concentration into the reactor, kgmol/ m^3
C_k type *k* active specie concentration, kgmol/m^3
C_p potential site concentration, kgmol/m3
CP
w cooling water specific heat, J/kgK
Df discharge factor
    dead polymer chain concentration with ***n*** monomers
$Dk n$ originated from site *k*, kgmol/m^3
DPI polydispersity index
K two-site equilibrium constant, kgmol^{-1}
    kinetic constant for reaction *r* with end-group *i* and
Kr,ik site *k*
$mC_3,$
f monomer feed flow rate, kg/s

mC
AT, f catalyst feed flow rate, kg/s
MFI melt flow index, gr/10 min
Mj component *j* molecular weight, kg/kgmol
    number average molecular weight for bulk polymer,
Mn kg/kgmol
Mw mass average molecular weight, kg/kgmol
    vector containing the number of each monomer

N in a polymer chain
NC number of liquid-phase components
Greek letters
    equilibrium constant for *j* component
γj between liquid phase and amorphous polymer phase
    ratio between solid-phase components concentration
ξ at reactor output flow and into reactor
    ratio between liquid-phase components concentration
η at reactor output flow and into reactor
    volume fraction of monomer in the amorphous
χ polymer phase
ρl liquid-phase density, kg m^3

REFERENCES

1. S. L. Bell, A private report by the Process Economics Program, SRI Consulting, IHS Inc., PEP Report 128E, September, 2011
2. A. G. M. Neto, J. C. Pinto, Steady-state modeling of slurry and bulk propylene polymerizations, *Chem. Eng. Sci.*, **56**, 4043 (2001).
3. T. F. Mckenna, J. Dupuy, R. Spitz, Modeling of transfer phenomena on heterogeneous Ziegler catalysts: Differences between theory and experiment in olefin polymerization, an introduction, *Appl. Polym. Sci.*, **57**, 371 (1995).
4. W. K. A. Shaffer, W. H. Ray, Polymerization of olefins through heterogeneous catalysis. XVIII. A kinetic explanation for unusual effects, *Appl. Polym. Sci.*, **65**, 1053 (1997).
5. P. Sarkar, S. K. Gupta, Steady state simulation of continuous -flow stirred - tank slurry propylene polymerization reactors, *Polym. Eng. Sci.,* **32**, 732 (1992).

6. P. Sarkar, S. K. Gupta, Dynamic simulation of propylene polymerization in continuous flow stirred tank reactors**,** *Polym. Eng. Sci.,* **33**, 368 (1993).
7. P. Sarkar**,** S. K. Gupta, Modelling of propylene polymerization in an isothermal slurry reactor, *Polymer*, **32** (15), 2842 (1991).
8. Zh. H. Luo, Y. Zheng, Z. K. Cao, S. H. Wen, Mathematical modeling of the molecular weight distribution of polypropylene produced in a loop reactor**,** *Polymer Engineering and Science*, **47** (10), 1643 (2007).
9. A. S. Reginato, J. J. Zacca, A. R. Secchi, Modeling and simulation of propylene polymerization in nonideal loop reactors, *AIChE Journal*, **49** (10), 2642 (2003).
10. I. van Putten, Polypropylene Polymerization in A Circulating Slugging Fluidized Bed Reactor, PhD thesis, Enschede, University of Twente, 2004.
11. C. Chatzidoukas, J. D. Perkins, E. N. Pistikopoulos, C. Kiparissides, Optimal grade transition and selection of closed-loop controllers in a gas-phase

olefin polymerization fluidized bed reactor; *Chemical Engineering Science*, **58**, 3643 (2003).

12. J. J. C. Samson, J. B. Bosman, G. Weickert, K. R. Westerterp, Liquid-phase polymerization of propylene with a highly active Ziegler-Natta catalyst. Influence of hydrogen, co-catalyst, and electron donor on reaction kinetics. *Journal of Polymer Science: Part A: Polymer Chemistry*, **37**, 219 (1999.

13. J. T. M. Pater, G. Weickert, W. P. M. van Swaaij, Polymerization of liquid propylene with a fourth generation ziegler-natta catalyst: influence of temperature, hydrogen, monomer concentration, and prepolymerization method on polymerization kinetics, *Journal of Applied Polymer Science*, **87**, 1421 (2003).

14. F. Shimizu, J. T. M. Pater, W. P. M. van Swaaij, G. Weickert, Kinetic study of a highly active MgCl2-supported Ziegler-Natta catalyst in liquid pool propylene polymerization. II. The influence of alkyl aluminum and alkoxysilane on catalyst activation and deactivation. *Journal of Applied Polymer Science*, **83**, 2669 (2002).

15. A. M. Al-haj, B. Betlem, B. Roffel, G. Weickert, Hydrogen response in liquid propylene polymerization: towards a generalized model, *AIChE Journal*, **52** (5) ,1866 (2006).

16. E. Albizzati, U. Gianinni, G. Collina, L. Noristi, L. Resconi, Polypropylene Handbook, Catalysts and Polymerizations, E. Moore (ed.), Chap. 3, Carl Hanser Verlag, 1996, p. 11.

17. G. Guastalla, U. Gianinni, The Influence of hydrogen on the polymerization of propylene and ethylene with an MgCl2 supported catalyst. *Makromol. Chem., Rapid Commun.* **4**,519 (1983).

18. R. Spitz, P. Masson, C. Bobichon, A. Guyot, Activation of propene polymerization by hydrogen for improved MgCl2-supported Ziegler-Natta catalysts, *Makromol. Chem.,* **190**, 717 (1989).

19. L. A. Rishina, E. I. Vizen, L. N. Sosnovskaja, F. S. Dyachkovsky, Study of the effect of hydrogen in propylene polymerization with MgCl2 supported Ziegler-Natta catalysts. Part 1, Kinetics of Polymerization, *European Polymer Journal*, **30** (11), 1309 (1994).

20. J. B. P. Soares, A. Hamielec, Kinetics of propylene polymerization with a non-supported heterogeneous Ziegler-Natta catalyst-effect of hydrogen on rate of polymerization, stereoregularity, and molecular weight distribution, *Polymer*, **37** (20), 4607 (1996).

21. G. C. Han-Adebekun, M. Hamba, W. H. Ray, kinetic study of gas phase olefin polymerization with a TiCl4/ MgCl2 catalyst. I. Effect of polymerization conditions. *Journal of Polymer Science: Part A: Polymer Chemistry*, **35**, 2063 (1997).

22. H. Mori, M. Endo, M. Terano, Deviation of hydrogen response during propylene polymerization with various Ziegler-Natta catalysts, *Journal of Molecular Catalysis A,* 211 (1999).

23. G. B. Meier, G. Weickert, W. P. M. van Swaaij, Gas-phase polymerization of propylene: reaction kinetics and molecular weight distribution, *Journal of Polymer Science*: *Part A: Polymer Chemistry* **39**(4), 500 (2001).

24. K. Soga, T. Siano, Effect of hydrogen on the molecular weight of polypropylene with Ziegler-Natta catalysts. *Polymer Bulletin*, **8**, 261 (1982).

25. , R. Kahrman, M. Erdogan, T. Bilgic, Polymerization of propylene using a prepolymerized high-active Ziegler-Natta catalyst. I. Kinetic studies. *Journal of Applied Polymer Science*, **60**, 333 (1996).

26. X.F. Yang, T. Zheng, L.M. Che, Zh.H. Luo, A dynamically distributed reactor model for identifying the flow fields in industrial loop propylene polymerization reactors, *J. Appl. Polym. Sci.*, 4302 (2013).

27. Y.-P. Zhua, Zh.-H. Luoa, J. Xiaoc, Multi-scale product property model of polypropylene produced in a FBR: From chemical process engineering to product engineering, *Computers and Chemical Engineering*, **71**, 39 (2014).

28. Sh. H. Kim, S. W. Baek, J. Ch. Lee, W. J. Lee, S. U. Hong , M. Oh, Dynamic simulation of liquid polymerization reactors in Sheripol process for polypropylene, *Journal of Industrial and Engineering Chemistry*, **33**,298 (2016).

29. G. M. N. Costa, S. Kislansky, L. C. Oliveira, F. L. P. Pessoa, S. A. B. Vieira de Melo, M. Embiruc, Modeling of solid–liquid equilibrium for polyethylene and polypropylene solutions with equations of state, *Journal of Applied Polymer Science*, **121**, 1832 (2010).

30. V. Busico, R. Cipullo, P. Corradini, Ziegler-Natta oligomerization of 1-alkenes: A Catalyst's "Fingerprint", 1. *Macromolecular Chemistry and Physics* **194**, 1079 (1993).

31. J. C. Chadwick, A. Miedema, O. Sudmeijer, Hydrogen Activation in Propene Polymerization with MgCl2 Supported Ziegler-Natta Catalysts: The Effect of the External Donor. *Macromolecular Chemistry and Physics,* **195**, 167 (1994).

32. H. G. Yuan, T. W. Taylor, K. Y. Choi, W. H. Ray, Polymerization of olefins through heterogeneous catalysis. 1. Low pressure propylene polymerization in slurry with Ziegler-Natta catalysts, *Journal of Applied Polymer Science,* **27**, 1691 (1982).

ОПТИМИЗИРАНЕ НА СВОЙСТВАТА НА КРАЙНИЯ ПРОДУКТ И ЕФЕКТИВНОСТ НА ЦИГЛЕР-НАТА КАТАЛИЗАТОР В ПРИСЪСТВИЕ И ОТСЪСТВИЕ НА ВОДОРОД ПРИ ПОЛИМЕРИЗАЦИЯТА НА ПРОПИЛЕН ЧРЕЗ КИНЕТИЧНО МОДЕЛИРАНЕ

Г. Х. Варшуе[1], А. Хейдаринасаб[1*] А. Вазири[1], Б. Розбахани[2]

[1] *Департамент по инженерна химия, Техерански научен и изследователски клон, Ислямски Азад университет, Техеран, Иран*

[2] *Департамент по химична и биомолекулярна техника, Изследователски партньор на университета "Райс", САЩ*

(Резюме)

С уникалната си сложност, кинетиката на полимеризацията има определящо влияние върху свойствата на крайния продукт, но силно се влияе от количеството на водород. Водородът, като агент на прехвърлянето на веригата, води до намаляване на средното молекулно тегло на полимера и директно влияе върху свойствата на крайния продукт; от друга страна, на основата на някои теории, води до известно нарастване на броя на активните центрове, последвано от намаляване. Следователно, това двойствено отнасяне трябва да се оптимизира. Досега не е разработен адекватен кинетичен модел за предсказване и оптимизиране на това отнасяне и за изчисляване на важните индекси на крайните продукти като индекс на потока на стопилката, бройно/средно молекулно тегло, индекс на полидисперсност. Освен определянето на тези индекси, чрез използване на модела могат да се изчислят някои основни кинетични параметри като активираща енергия, първоначална скорост на реакцията и константа на деактивация. Предлаганият в тази работа модел е кодиран в MATLAB/SIMULINK софтуер с използване на подхода за полимерен моментен баланс, основаващ се на теорията за спящите центрове като най-достоверна теория до момента. Моделът е валидиран чрез сравняване с лабораторни експериментални данни, като е установено съвпадение в рамките на приемливата грешка. Намерени са оптималната реакционна температура (70°С) и оптималното количество водород (18 mg) в съответствие с използвания катализатор.